

A Landau–de Gennes theory for twist-bend and splay-bend nematic phases of colloidal suspensions of bent rods

Cite as: J. Chem. Phys. **152**, 224502 (2020); <https://doi.org/10.1063/5.0008936>

Submitted: 26 March 2020 . Accepted: 17 May 2020 . Published Online: 08 June 2020

Carmine Anzivino , René van Roij , and Marjolein Dijkstra 



View Online



Export Citation



CrossMark

ARTICLES YOU MAY BE INTERESTED IN

[Inverse methods for design of soft materials](#)

The Journal of Chemical Physics **152**, 140902 (2020); <https://doi.org/10.1063/1.5145177>

[Dynamics of poly\[n\]catenane melts](#)

The Journal of Chemical Physics **152**, 214901 (2020); <https://doi.org/10.1063/5.0007573>

[Surveying the free energy landscape of clusters of attractive colloidal spheres](#)

The Journal of Chemical Physics **152**, 134901 (2020); <https://doi.org/10.1063/1.5144984>

Lock-in Amplifiers
up to 600 MHz



Watch



A Landau–de Gennes theory for twist-bend and splay-bend nematic phases of colloidal suspensions of bent rods

Cite as: J. Chem. Phys. 152, 224502 (2020); doi: 10.1063/5.0008936

Submitted: 26 March 2020 • Accepted: 17 May 2020 •

Published Online: 8 June 2020



View Online



Export Citation



CrossMark

Carmine Anzivino,^{1,a)} René van Roij,² and Marjolein Dijkstra^{1,b)}

AFFILIATIONS

¹Soft Condensed Matter, Debye Institute for Nanomaterial Science, Utrecht University, Princetonplein 1, Utrecht 3584 CC, The Netherlands

²Institute for Theoretical Physics, Center for Extreme Matter and Emergent Phenomena, Utrecht University, Princetonplein 5, Utrecht 3584 CC, The Netherlands

^{a)}Author to whom correspondence should be addressed: c.anzivino@uu.nl

^{b)}Electronic mail: m.dijkstra@uu.nl

ABSTRACT

We develop a phenomenological Landau–de Gennes (LdG) theory for lyotropic colloidal suspensions of bent rods using a Q-tensor expansion of the chemical-potential dependent grand potential. In addition, we introduce a bend flexoelectric term, coupling the polarization and the divergence of the Q-tensor, to study the stability of uniaxial (N), twist-bend (N_{TB}), and splay-bend (N_{SB}) nematic phases of colloidal bent rods. We first show that a mapping can be found between the LdG theory and the Oseen–Frank theory. By breaking the degeneracy between the splay and bend elastic constants, we find that the LdG theory predicts either an N – N_{TB} – N_{SB} or an N – N_{SB} – N_{TB} phase sequence upon increasing the particle concentration. Finally, we employ our theory to study the first-order N – N_{TB} phase transition, for which we find that K_{33} as well as its renormalized version K_{33}^{eff} remain positive at the transition, whereas K_{33}^{eff} vanishes at the nematic spinodal. We connect these findings to recent simulation results.

Published under license by AIP Publishing. <https://doi.org/10.1063/5.0008936>

I. INTRODUCTION

Bent-core liquid crystals are mesophases formed by molecules with a “banana-like” shape.¹ In the simplest liquid-crystal phase, i.e., the uniaxial nematic (N) phase, the long axes of the bent-core molecules are preferentially aligned along a common direction, the so-called nematic director \hat{n} , and the transverse orientations of the molecules are randomly oriented in the plane perpendicular to \hat{n} . In addition to the N phase with an orientational order of the main molecular axis, the molecular shape can stabilize a nematic phase with polar order, in which the transverse orientations exhibit a net alignment in a direction perpendicular to \hat{n} . In 1969, Meyer² argued that the polar order of the transverse directions couples to the bend deformations of the nematic director \hat{n} through a mechanism called the *bend flexoelectric effect*. The polar order and the bend flexoelectric effect may occur in liquid crystals due to electrostatic polarization and may also arise due to the molecular shape in systems of

bent-core molecules in the absence of electric fields. As a result, it is particularly easy to induce bend deformations in the nematic director field of bent-core liquid crystals. Many years later, Dozov³ noted that the bend elastic constant K_{33} can be very small for bent-core liquid crystals, yielding a low energy cost for bend deformations. In addition, Dozov speculated that K_{33} could also become negative in certain bent-core liquid crystals. In this case, higher-order terms in the derivatives of the nematic director field (beyond linear elasticity) should be included in the free energy in order to stabilize the system. The competition between the putative negative K_{33} term and the positive higher-order terms would favor spontaneous bend deformations. Interestingly, however, the theoretical work of Dozov did not consider any polar order. Since it is impossible to extend a pure bend deformation in three-dimensional space, Meyer as well as Dozov predicted that the uniaxial N phase can become unstable with respect to either a spatially modulated twist-bend nematic (N_{TB}) phase, characterized by a heliconical variation with bend and

twist deformations in the molecular orientation [see Fig. 1(a)], or a modulated splay-bend nematic (N_{SB}) phase, characterized by alternating domains of splay and bend^{3,4} [see Fig. 1(b)]. Quantitatively, Dozov's theory, based on the Oseen–Frank elastic theory, predicts that the uniaxial N phase becomes unstable to the formation of N_{TB} or N_{SB} phases at a critical point corresponding to $K_{33} = 0$, where the system either stabilizes an N_{TB} phase if $K_{11} > 2K_{22}$ or an N_{SB} phase if $K_{11} < 2K_{22}$, with K_{11} and K_{22} being the splay and twist elastic constants, respectively.³

Recently, Selinger and collaborators^{5–7} suggested that the presence of polar order could provide the simplest explanation not only for the formation of spatially modulated phases, in agreement with Meyer, but also for the negative bend elastic constant K_{33} proposed by Dozov. These authors introduced a Landau theory that combines the Oseen–Frank free energy for the nematic director \hat{n} , the polar order \mathbf{P} perpendicular to \hat{n} , and the coupling between the polar order and bend deformations. By minimizing the free energy with respect to the polar order, they obtained Dozov's effective free energy in terms of only the nematic director field \hat{n} with renormalized elastic constants. In this picture, K_{33} remains always positive, while its renormalized version K_{33}^{eff} decreases in magnitude and vanishes at a critical point where the uniaxial N phase becomes unstable with respect to the N_{TB} or N_{SB} phase. Interestingly, they also found the same criterion for the relative stability of the spatially modulated phases calculated by Dozov,⁶ i.e., $K_{11} < 2K_{22}$ for an N_{SB} phase and $K_{11} > 2K_{22}$ for an N_{TB} phase. Finally, Selinger's theory has been extended^{8–12} to a mesoscopic Landau–de Gennes (LdG) theory where the director \hat{n} is replaced by a second rank, symmetric, and traceless tensor $\mathbf{Q}(\mathbf{r})$ with components $Q_{\alpha\beta}(\mathbf{r})$, where $\alpha, \beta = 1, 2, 3$ represent the Cartesian coordinates.

For completeness, we also mention that theories have been developed for bent-core liquid crystals that do not involve spontaneous polar order or a negative bend elastic constant.^{13–18} Additionally, molecular field approaches^{19–30} for bent-core liquid crystals exist, of which several^{20,26,28–30} support the idea of softening of the

bend elastic constant before the onset of the polar order in bent-core liquid crystals, in agreement with Selinger *et al.*^{5–7}

Much research in recent years has been focused on thermotropic bent-core mesogens that become liquid crystalline upon lowering the temperature. Very recently, various routes have been developed to synthesize lyotropic colloidal model systems of bent-core molecules, e.g., silica rods with a sharp kink^{31–33} or smoothly curved SU-8 rods.³⁴ The liquid crystalline behavior of these colloidal systems is driven by concentration and has been studied by simulations and microscopic theories. Using Onsager theory,³⁵ a first-order uniaxial N to N_{TB} phase transition has been predicted recently in a system of hard curved particles at sufficiently high particle concentrations,¹⁹ which has been confirmed in computer simulations^{19,36} on systems of hard bent spherocylinders. In addition, this simulation study showed that the N – N_{TB} phase transition is followed by a second-order N_{TB} – N_{SB} phase transition in a polydisperse system of hard bent spherocylinders and in a system of hard curved particles.

In this paper, we extend the existing LdG theories of thermotropic bent-core liquid crystals to lyotropic liquid crystals in order to develop a framework to describe the recent findings of Refs. 19 and 36. To this end, we introduce a chemical-potential dependent grand potential based on a Q -tensor expansion and a bend flexoelectric term coupling the polarization and the divergence of the Q -tensor.^{8–12} We first show that a mapping can be found between the LdG theory and the Oseen–Frank theory of Selinger and coworkers.^{6,7} We then show, by breaking the degeneracy between the splay and bend elastic constants, that the LdG theory predicts a series of second-order phase transitions between periodically modulated nematic phases, reproducing what was found in Ref. 36. Finally, we employ our theory to study the first-order N – N_{TB} phase transition observed in simulations. We find that while the LdG theory predicts that $K_{33} > 0$ and $K_{33}^{\text{eff}} = 0$ at a second-order N – N_{TB} phase transition, it also predicts that K_{33} as well as K_{33}^{eff} remains positive at a first-order N – N_{TB} transition, whereas K_{33}^{eff} vanishes at the nematic spinodal.

As a final introductory remark, it is worth mentioning that the splay-bend nematic phase considered in this paper differs from the so-called splay nematic (N_S) phase considered in Refs. 12, 37, and 38. This N_S phase is characterized by a modulation perpendicular to the average director, while the N_{SB} phase is characterized by a spatial modulation parallel to the global nematic director. Moreover, the onset of the N_S phase is driven by softening of the renormalized splay elastic constant K_{11}^{eff} rather than of the renormalized bend elastic constant K_{33}^{eff} .

The outline of this paper is as follows: Sec. II describes our LdG theory. In Sec. III, we briefly review the isotropic-nematic phase transition of hard rods within this framework, which will be used as a reference system throughout this paper. In Sec. IV, we investigate possible phase sequences of the spatially modulated phases. The first-order N – N_{TB} transition is studied in Sec. V, and the renormalized elastic constants are derived in Sec. VI. Finally, we present our conclusions and a discussion in Sec. VII.

II. LANDAU–de GENNES THEORY

LdG theory is based on the hypothesis that equilibrium properties of a thermodynamic system can be found from a variational

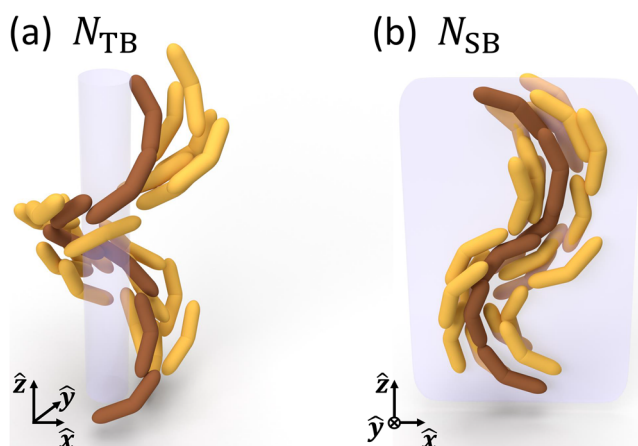


FIG. 1. (a) Twist-bend nematic (N_{TB}) phase characterized by a helical variation of the particle orientation along the z -axis. (b) Splay-bend nematic (N_{SB}) phase characterized by alternating domains of splay and bend in the x - z plane.

Helmholtz (or Gibbs) free energy F , constructed as an expansion in powers of a suitable order parameter. A restriction on the expansion is that it must be stable against an unlimited growth of the order parameter. It is well known³⁹ that the orientational order of three-dimensional nematic liquid crystals can be described by a second-rank, symmetric, traceless tensor field, $\mathbf{Q}(\mathbf{r})$, with cartesian components $Q_{\alpha\beta}(\mathbf{r})$ for $\alpha, \beta = 1, 2, 3$, which vanishes in the isotropic (I) phase and thus serves as an order parameter for the N phase. The eigenvector of \mathbf{Q} corresponding to the maximum modulus of a non-degenerate eigenvalue defines the nematic director $\hat{\mathbf{n}}$ of the system. The variational LdG free energy F for ordinary, non-chiral nematics is constructed from frame-invariant contractions of $Q_{\alpha\beta}$ and spatial derivatives $\partial_\lambda Q_{\alpha\beta}$ such as $Q_{\alpha\beta}Q_{\beta\alpha}$, $Q_{\alpha\beta}Q_{\beta\lambda}Q_{\lambda\alpha}$, with phenomenological coefficients that contain the dependence on the thermodynamic state (pressure and temperature). Usually for thermotropic liquid crystals, only the quadratic term of the Landau expansion changes sign as a function of temperature, which drives the phase transition.^{40–42}

In contrast to “ordinary” nematics, a proper characterization of orientational order exhibited by bent-core liquid-crystal phases requires additional order parameters. In the case of theories based on the flexoelectric effect, not only the tensor field $\mathbf{Q}(\mathbf{r})$ is required but also a vector field $\mathbf{P}(\mathbf{r})$ with cartesian components $P_\alpha(\mathbf{r})$ that describes the polar order in a direction perpendicular to $\hat{\mathbf{n}}$. In the I phase, $\mathbf{Q} = \mathbf{0}$ and $\mathbf{P} = \mathbf{0}$; in the uniaxial N phase, $\mathbf{Q} \neq \mathbf{0}$ and $\mathbf{P} = \mathbf{0}$; and in the spatially modulated nematic phases, $\mathbf{Q} \neq \mathbf{0}$ and $\mathbf{P} \neq \mathbf{0}$. General $O(3)$ -symmetric extensions of the free energy F that contain additionally lowest order couplings with \mathbf{P} and its derivatives $\partial_\alpha P_\beta$ have been developed in Refs. 8–12. However, these expansions are only suitable for thermotropic systems that become liquid crystalline as a function of temperature. In contrast, lyotropic systems become ordered as a function of density and are not conveniently described by the Helmholtz free energy F . A naive remedy for this problem would be to replace the temperature in F by the density ρ , but this cannot capture the density jumps that are found at first-order transitions, which for the I – N phase transition can be as large as 25%.⁴³ The density discontinuity at the I – N transition is instead exhibited by microscopic theories, such as Onsager theory.

Here, we follow Ref. 44 and set up a Landau expansion for lyotropics for which we will use the grand potential Ω rather than the Helmholtz (or Gibbs) free energy F . By using Ω , the expansion parameters will depend on the chemical potential μ , and the density jumps will naturally be encoded through the relation $\partial(\Omega/V)/\partial\mu|_{V,T} = -\rho$, with V being the volume of the system and ρ being the average density. Only the quadratic term $Q_{\alpha\beta}Q_{\beta\alpha}$ has a μ -dependent prefactor that changes sign to drive the phase transition. This procedure is easier to use than, for example, the phase-field-crystal method of Ref. 45, which produces terms that also explicitly depend on density, for which also an Euler–Lagrange equation for ρ needs to be solved, in addition to the one for \mathbf{Q} .

We consider a system of hard bent rods modeled as curved or kinked rods of contour length L and diameter D , at chemical potential μ in a macroscopic volume V at fixed temperature T . We write the LdG grand potential as

$$\Delta\Omega(\mathbf{Q}, \mathbf{P}) = \int_V d\mathbf{r} [\Delta\omega_b + \omega_e + \omega_p], \quad (1)$$

where $\Delta\omega_b \equiv \Delta\omega_b(\mathbf{Q}; \mu)$ is the excess bulk grand potential density with respect to the I state, $\omega_e \equiv \omega_e(\mathbf{Q}, \nabla\mathbf{Q})$ describes elastic deformations and surface tension effects, and $\omega_p \equiv \omega_p(\mathbf{Q}, \mathbf{P}, \nabla\mathbf{Q}, \nabla\mathbf{P})$ contains additionally lowest order couplings between \mathbf{Q} and the polarization field \mathbf{P} and its derivatives $\partial_\alpha P_\beta$.

We expand the bulk contribution in units of $\beta^{-1} = k_B T$ with k_B being the Boltzmann constant, until fourth order in \mathbf{Q} , which gives us

$$\beta B_2 \Delta\omega_b(\mathbf{Q}; \mu) = \frac{2}{3} a \beta (\mu^* - \mu) Q_{\alpha\beta} Q_{\beta\alpha} - \frac{4}{3} b Q_{\alpha\beta} Q_{\beta\lambda} Q_{\lambda\alpha} + \frac{4}{9} d Q_{\alpha\beta} Q_{\beta\alpha} Q_{\lambda\mu} Q_{\mu\lambda}, \quad (2)$$

where we use Einstein’s summation convention for repeated indices throughout this paper. The second virial coefficient in the isotropic fluid phase is given by $B_2 = \pi L^2 D/4$ in the limit $L \gg D$ and is included in our definition to render the Landau coefficients a , b , and d conveniently dimensionless. For simplicity, we assume them to be independent of μ . We also introduce μ^* , the chemical potential at which the quadratic term changes sign, i.e., it defines the spinodal of the I – N transition. A stable I phase at $\mu < \mu^*$ requires $a > 0$, the stability of expansion (2) with respect to an unlimited growth of \mathbf{Q} requires that $d > 0$, while $b > 0$ allows us to describe a first-order I – N transition to a state with $\mathbf{Q} \neq \mathbf{0}$. Throughout, we will satisfy these stability criteria.

For the terms in gradients of \mathbf{Q} , we only retain terms up to the square gradients in \mathbf{Q} , and we consider only one of the possible invariants that involve the coupling between the order parameter \mathbf{Q} and quadratic gradient in \mathbf{Q} to break the degeneracy between the splay and bend elastic constants K_{11} and K_{33} .⁴⁶ We thus write

$$\beta B_2 \omega_e(\mathbf{Q}, \nabla\mathbf{Q}) = \frac{2}{9} l_1 (\partial_\alpha Q_{\beta\lambda})(\partial_\alpha Q_{\beta\lambda}) + \frac{2}{9} l_2 (\partial_\alpha Q_{\alpha\lambda})(\partial_\beta Q_{\beta\lambda}) - \frac{2}{9} l_3 Q_{\alpha\beta} (\partial_\gamma Q_{\alpha\gamma})(\partial_\xi Q_{\beta\xi}), \quad (3)$$

where we omitted another second-order term in $\nabla\mathbf{Q}$, which scales with $(\partial_\alpha Q_{\beta\lambda})(\partial_\lambda Q_{\beta\alpha})$ because it can be written as a linear combination of a surface term and the elastic terms already included in the expansion (3). We express the expansion parameters l_1 , l_2 , and l_3 in units of L^2 throughout this paper. We note again that we have chosen only one of the possible couplings between \mathbf{Q} and $\nabla\mathbf{Q}$ to break the degeneracy between K_{11} and K_{33} .⁴⁶ This choice is arbitrary; in addition, other terms could have been considered or even more terms could have been included. Since all couplings add a contribution proportional to S^3 to the elastic constants, the predictions of the theory are not affected by this choice.

Expressing $\mathbf{Q}(\mathbf{r})$ in terms of a scalar order parameter $S(\mathbf{r})$ and a nematic director field $\mathbf{n}(\mathbf{r})$,

$$Q_{\alpha\beta}(\mathbf{r}) = \frac{3}{2} S(\mathbf{r}) \left(n_\alpha(\mathbf{r}) n_\beta(\mathbf{r}) - \frac{1}{3} \delta_{\alpha\beta} \right), \quad (4)$$

we can relate the parameters l_1 , l_2 , and l_3 to the Oseen–Frank elastic constants through $\beta DK_{11} = 4S^2(2l_1 + l_2 - Sl_3)/(\pi L^2)$, $\beta DK_{22} = 8S^2 l_1/(\pi L^2)$, and $\beta DK_{33} = 4S^2(2l_1 + l_2 + (S/2)l_3)/(\pi L^2)$, respectively. These relations can be found by comparing the elastic expansion (3) using expression (4) with the Oseen–Frank elastic

energy,^{47,48}

$$F = \frac{1}{2} \int d\mathbf{r} [K_{11}(\nabla \cdot \hat{\mathbf{n}})^2 + K_{22}(\hat{\mathbf{n}} \cdot \nabla \times \hat{\mathbf{n}})^2 + K_{33}|\hat{\mathbf{n}} \times (\nabla \times \hat{\mathbf{n}})|^2], \quad (5)$$

where K_{11} , K_{22} , and K_{33} are the splay, twist, and bend elastic constants, respectively. We assume l_1 , l_2 , and l_3 to be independent of μ .

Finally, we expand ω_P up to sixth order in \mathbf{P} and write

$$\begin{aligned} \beta B_2 \omega_P(\mathbf{Q}, \mathbf{P}, \nabla \mathbf{Q}, \nabla \mathbf{P}) = & e_2 P_\alpha \left(\delta_{\alpha\beta} + \frac{2}{S_0} Q_{\alpha\beta} \right) P_\beta \\ & + e_4 P_\alpha P_\alpha P_\beta P_\beta - \lambda P_\alpha (\partial_\beta Q_{\alpha\beta}) \\ & + \kappa (\partial_\alpha P_\beta) (\partial_\alpha P_\beta) + e_6 P_\alpha P_\alpha P_\beta P_\beta P_\gamma P_\gamma, \quad (6) \end{aligned}$$

with coefficients e_2 , e_4 , e_6 , κ , λ , and S_0 . Throughout this paper, we will express λ and κ in terms of L and L^2 , respectively. Stability in the dilute limit requires $e_2 > 0$, while stability with respect to an unlimited growth of \mathbf{P} requires $e_6 > 0$. The coefficients $2/S_0$, λ , and κ represent the strength of the coupling between \mathbf{Q} and \mathbf{P} fields, the flexoelectric coupling between \mathbf{P} and gradients in \mathbf{Q} , and a polar elastic constant, respectively. In order to describe a favored polarization perpendicular to the nematic director, leading to bend flexoelectricity, we set $S_0 > 0$.⁸ Finally, we allow e_4 to be positive as well as negative.

Our LdG expansion is very similar to those of Refs. 8 and 11. Nevertheless, in contrast to their work, and following the suggestion of Ref. 7, we consider terms up to sixth order in \mathbf{P} and simultaneously allow the coefficient e_4 of the fourth-order term in \mathbf{P} to be either positive or negative. This choice allows us to describe first-order as well as second-order transitions to the spatially modulated phases.⁴⁹ In particular, if $e_4 < 0$, we expect first-order phase transitions, while if $e_4 \geq 0$, we expect second-order phase transitions. Our expansion includes the additional elastic term $Q_{\alpha\beta}(\partial_\gamma Q_{\alpha\gamma})(\partial_\xi Q_{\beta\xi})$ to break the degeneracy between the splay and bend elastic constants K_{11} and K_{33} in agreement with Ref. 37. However, we note that Ref. 37 lacks the term $(\partial_\alpha Q_{\alpha\lambda})(\partial_\beta Q_{\beta\lambda})$ and only considers terms up to second-order in \mathbf{P} . We also remark that our additional elastic term not only allows us to break the degeneracy between the splay and bend elastic constants but also enables us to change the ratio between the splay and twist elastic constants K_{11}/K_{22} by varying the particle concentration. As will become clear in Sec. IV, this latter condition is important for investigating the possibility of concentration-driven phase transitions between the periodically modulated phases, as was recently found in simulations of hard particles.³⁶

III. I-N TRANSITION

Here, we briefly review the LdG theory to describe the I - N transition of uniaxial hard rods as derived in Ref. 44. As stated in Sec. II, the uniaxial N phase is characterized by $\mathbf{Q} \neq \mathbf{0}$ and $\mathbf{P} = \mathbf{0}$, and hence, the ω_P term in the grand potential (1) vanishes. We describe the bulk uniaxial N phase by taking $\hat{\mathbf{n}}$ parallel to the z -axis. In this case, the elastic expansion $\omega_e = 0$ and $\Delta\Omega/V$ reduces to $\Delta\omega_b$. Inserting the tensor order parameter (4) with $\hat{\mathbf{n}} = (0, 0, 1)$ in (2), we obtain $\beta B_2 \Delta\omega_b = a\beta(\mu^* - \mu)S^2 - bS^3 + dS^4$. The Euler-Lagrange equation $\partial\Delta\omega_b/\partial S = 0$ can be solved analytically, in order to find the stable, metastable,

and unstable phases. We find the solutions

$$\begin{aligned} S_I(\mu) &= 0; \\ S_N^\pm(\mu) &= \frac{3b}{8d} \left(1 \pm \sqrt{1 - \frac{32ad\beta(\mu^* - \mu)}{9b^2}} \right), \quad (7) \end{aligned}$$

whose stability can be investigated by analyzing the sign of $\partial^2\Delta\omega_b/\partial S^2$. We first note that from the conditions $\partial^2\Delta\omega_b/\partial S^2|_{S=S_I} = 0$, $\partial^2\Delta\omega_b/\partial S^2|_{S=S_N^\pm} = 0$ and $\Delta\omega_b(S_I) = \Delta\omega_b(S_N^\pm)$, we can find the chemical potential μ^* corresponding to the spinodal of the I phase with respect to the N phase, the chemical potential $\beta\mu^+ = \beta\mu^* - 9b/(32ad)$ corresponding to the spinodal of the N phase with respect to the I phase, and the chemical potential $\beta\mu_{IN} = \beta\mu^* - b^2/(4ad)$ corresponding to the I - N transition, respectively. We then find that (i) for $\mu < \mu^+$, the I phase (S_I) is the stable configuration; (ii) for $\mu^+ < \mu < \mu_{IN}$, the I phase is stable, S_N^- is unstable, and S_N^+ is metastable; (iii) for $\mu_{IN} < \mu < \mu^*$, the S_N^+ solution is stable, the I phase is metastable, and S_N^- is unstable; and (iv) for $\mu > \mu^*$, the S_N^+ solution is stable, S_N^- is metastable, and the I phase is unstable. The solution S_N^+ represents the N phase, and for the sake of simplicity, we will use $S_N(\mu) \equiv S_N^+(\mu)$ throughout this paper.

In order to describe the I - N transition of hard rods, we first convert the chemical potential μ to the particle concentration $c = B_2\rho$ and then fit the phenomenological coefficients a , b , and d to results from Onsager theory.⁴⁴ Concerning the first, we introduce the grand potential density of the I state ω_I and define $\omega \equiv \omega_I + \Delta\omega_b$. From the condition $\partial(B_2\omega)/\partial\mu = -c$, we then find

$$c(\mu) = c_I(\mu) + aS^2(\mu), \quad (8)$$

where the particle concentration of the I phase $c_I(\mu) = -\partial(B_2\omega_I)/\partial\mu$ can be calculated within Onsager theory, by using an isotropic distribution function, such that $\beta\mu(c_I) = \log(c_I/4\pi) + 2c_I$.⁵⁰ By inverting this relation, we obtain $c_I(\mu)$. For the fit of the phenomenological coefficients a , b , and d , we exploit the thermodynamic quantities of the system at the I - N phase coexistence. Using Onsager theory for a system of hard rods in the limit $L/D \rightarrow \infty$,^{50,51} we find $c_I(\mu_{IN}) = 3.290$, $c(\mu_{IN}) = 4.191$, $\beta\mu^* = 6.855$, $\beta\mu_{IN} = 5.241$, and $S_{IN} = 0.7992$. Inserting these values into the following expressions:

$$\begin{aligned} c(\mu_{IN}) &= c_I(\mu_{IN}) + aS_{IN}^2, \\ \beta\mu_{IN} &= \beta\mu^* - b^2/(4ad), \\ S_{IN} &= b/(2d), \quad (9) \end{aligned}$$

we obtain $a = 1.436$, $b = 5.851$, and $d = 3.693$. With this set of coefficients, a plot of S_I and S_N as a function of the concentration c as defined by Eq. (8) allows one to observe that the concentration jump associated with the I - N transition is correctly captured, as shown in Ref. 44. Unless stated otherwise, we will use these values of a , b , d , and μ^* in the following. We will also follow Ref. 44 in fitting the square-gradient coefficients l_1 and l_2 by using the surface tension of a planar I - N interface of a system of hard rods with a parallel and perpendicular anchoring, yielding $l_1 = 0.165L^2$ and $l_2 = 1.708L^2$. We thus take a system of hard rods with $L/D \rightarrow \infty$ as a reference system for our study. Alternative reference systems are straightforward to implement, provided that a sufficient number of quantities are known at the bulk I - N transition.

IV. SPATIALLY MODULATED PHASES

In this section, we study the phase behavior of lyotropic suspensions of bent rods by employing the LdG theory introduced in Sec. II with $e_6 = 0$ and $e_4 > 0$ in Eq. (6), i.e., using the formalism for second-order phase transitions. We show that if $l_3 \neq 0$ in Eq. (3), the LdG theory predicts that an $N-N_{TB}-N_{SB}$ and an $N-N_{SB}-N_{TB}$ phase sequence can be stabilized in this system upon increasing the nematic order, in addition to the $N-N_{TB}$ and $N-N_{SB}$ transitions already predicted by the same theory in the case of $l_3 = 0$.

To this end, we describe the N_{TB} phase by a nematic director $\hat{\mathbf{n}}_{TB}(z)$ precessing around the z -axis with a conical angle θ , a pitch $p = 2\pi/q$, and a polarization vector $\mathbf{P}_{TB}(z)$ perpendicular to $\hat{\mathbf{n}}_{TB}(z)$, given by^{3,6}

$$\begin{aligned}\hat{\mathbf{n}}_{TB}(z) &= (\sin\theta \cos(qz), \sin\theta \sin(qz), \cos\theta), \\ \mathbf{P}_{TB}(z) &= P(\sin(qz), -\cos(qz), 0).\end{aligned}\quad (10)$$

We describe the N_{SB} phase by a nematic director $\hat{\mathbf{n}}_{SB}(z)$ and polarization vector $\mathbf{P}_{SB}(z)$ given by^{3,6}

$$\begin{aligned}\hat{\mathbf{n}}_{SB}(z) &= (\sin\phi(z), 0, \cos\phi(z)), \\ \mathbf{P}_{SB}(z) &= P\psi(z)(-\cos\phi(z), 0, \frac{1}{2}\sin 2\phi(z)),\end{aligned}\quad (11)$$

where $\psi(z) = \cos(qz)$ and $\phi(z) = \theta \sin qz$. Observe that $\hat{\mathbf{n}}_{SB}$ describes alternating domains of splay and bend.

In order to study the stability of these phases, we first find the equilibrium values of q and θ , which can then be inserted into Eq. (1). Subsequently, we minimize the obtained Ω with respect to S and P at fixed μ , i.e., we solve the Euler–Lagrange equations $\partial\Delta\Omega/\partial S = 0$ and $\partial\Delta\Omega/\partial P = 0$. However, since we are considering second-order transitions from the uniaxial N phase, the dependence of S on μ is known analytically, given by the $S_N(\mu)$ solution of Eq. (7). As a consequence, we can perform the stability analysis by minimizing Ω with respect to P at fixed S , i.e., by solving the Euler–Lagrange equation $\partial\Delta\Omega/\partial P = 0$. The dependence of P and S on the particle concentration can finally be obtained from the dependence on μ using the procedure described in Sec. III.

A. Comparison with the Oseen–Frank theory

As already mentioned in the Introduction, the Oseen–Frank theory of Dozov³ and Selinger and co-workers^{6,7} predicts a phase transition from a uniaxial N phase to either an N_{TB} or an N_{SB} phase. In this subsection, we show that a complete mapping exists between the LdG theory with $l_3 = 0$, i.e., with a degenerate bend and splay elastic constant, and the Oseen–Frank theory of Selinger and co-workers.^{6,7}

To compute the grand potential density of the N_{TB} phase, we insert $\hat{\mathbf{n}}_{TB}(z)$ in the tensor order parameter [Eq. (4)] and the resulting $\mathbf{Q}(z)$ together with $\mathbf{P}_{TB}(z)$ in the grand potential [Eq. (1)]. We minimize the obtained grand potential with respect to the wave number q and the tilt angle θ , respectively, and find

$$q_{TB} = \frac{3\lambda \sin(2\theta_{TB})SP}{8\kappa P^2 + 4S^2(2l_1 + l_2) \sin^2\theta_{TB} - 4S^2l_2 \sin^4\theta_{TB}} \quad (12)$$

and

$$\sin^2\theta_{TB} = \frac{\kappa P^2}{S^2l_1} + \frac{\sqrt{\kappa P^2(\kappa P^2 + S^2l_1)}}{S^2l_1}. \quad (13)$$

Inserting Eqs. (12) and (13) back into Eq. (1) and approximating for small P , we find the grand potential density of the N_{TB} phase,

$$\begin{aligned}\frac{\Delta\Omega_{TB}}{V} &= \frac{\Delta\Omega}{V} - \frac{\Delta\Omega_N}{V} \\ &= \left[\frac{e_2(S_0 - S)}{S_0} - \frac{9\lambda^2}{8(2l_1 + l_2)} \right] P^2 \\ &\quad + \frac{9\lambda^2\sqrt{\kappa S^2l_1}}{2S^2(2l_1 + l_2)^2} |P|^3 + e_4P^4 + O(P^5),\end{aligned}\quad (14)$$

where $\Delta\Omega_N/V = aS^2(\mu^* - \mu) - bS^3 + dS^4$ is the grand potential density of the N phase.

Analogously, in order to compute the grand potential density of the N_{SB} phase, we insert the nematic director $\hat{\mathbf{n}}_{SB}(z)$ into the tensor order parameter [Eq. (4)] and the resulting $\mathbf{Q}(z)$ together with $\mathbf{P}_{SB}(z)$ into the grand potential [Eq. (1)]. In contrast to the case of the N_{TB} phase, the resulting grand potential density varies periodically as a function of z , and hence, we average it over a full period $2\pi/q$ to find

$$\frac{\Delta\Omega}{V} = \frac{q}{2\pi} \int_0^{2\pi/q} dz \Delta\omega(z). \quad (15)$$

We then minimize the obtained grand potential with respect to the wave number q and the tilt angle θ , respectively, and find

$$q_{SB} = \frac{3\lambda\theta_{SB}(\theta_{SB}^2 - 8)PS}{8(4 + 3\theta_{SB}^2)\kappa P^2 + 16S^2(2l_1 + l_2)\theta_{SB}^2} \quad (16)$$

and

$$\theta_{SB}^2 = \frac{16\kappa P^2}{3\kappa P^2 + \sqrt{\kappa P^2(57\kappa P^2 + 32S^2(2l_1 + l_2))}}. \quad (17)$$

Inserting Eqs. (16) and (17) back into Eq. (1) and approximating for small P , we find for the grand potential density of the N_{SB} phase,

$$\begin{aligned}\frac{\Delta\Omega_{SB}}{V} &= \frac{\Delta\Omega}{V} - \frac{\Delta\Omega_N}{V} \\ &= \left[\frac{e_2(S_0 - S)}{2S_0} - \frac{9\lambda^2}{16(2l_1 + l_2)} \right] P^2 \\ &\quad + \frac{9\lambda^2\sqrt{\kappa S^2(2l_1 + l_2)}}{8\sqrt{2}S^2(2l_1 + l_2)^2} |P|^3 + \frac{3e_4}{8} P^4 + O(P^5).\end{aligned}\quad (18)$$

We observe that for small P , both $\Delta\Omega_{TB}$ and $\Delta\Omega_{SB}$ vanish at the critical scalar nematic order parameter

$$S_c = S_0 \left(1 - \frac{9\lambda^2}{8e_2(2l_1 + l_2)} \right). \quad (19)$$

Close to this point, we can assume $P_{TB} \ll 9\lambda^2\sqrt{\kappa S^2l_1}/(2e_4S^2(2l_1 + l_2)^2)$ and $P_{SB} \ll 3\lambda^2\sqrt{\kappa S^2(2l_1 + l_2)}/(\sqrt{2}e_4S^2(2l_1 + l_2)^2)$ such that the cubic terms dominate over the quartic terms in Eqs. (14) and (18). Solving the Euler–Lagrange equations $\partial(\Delta\Omega_{TB}/V)/\partial P = 0$ and $\partial(\Delta\Omega_{SB}/V)/\partial P = 0$, we find

$$P_{TB} = \frac{4e_2S^2(2l_1 + l_2)^2(S - S_c)}{27S_0\lambda^2\sqrt{\kappa S^2l_1}} \quad (20)$$

and

$$P_{SB} = \frac{8\sqrt{2}e_2S^2(2l_1 + l_2)^2(S - S_c)}{27S_0\lambda^2\sqrt{\kappa S^2(2l_1 + l_2)}}, \quad (21)$$

respectively. Inserting Eqs. (20) and (21) back in Eqs. (14) and (18) yields

$$\frac{\Delta\Omega_{\text{TB}}}{V} = -\frac{16e_2^3 S^2 (2l_1 + l_2)^4 (S - S_c)^3}{729S_0^3 \kappa \lambda^4 l_1} \quad (22)$$

and

$$\frac{\Delta\Omega_{\text{SB}}}{V} = -\frac{64e_2^3 S^2 (2l_1 + l_2)^3 (S - S_c)^3}{729S_0^3 \kappa \lambda^4}. \quad (23)$$

The ratio between the grand potential densities (22) and (23) is then given by

$$\frac{\Delta\Omega_{\text{TB}}}{\Delta\Omega_{\text{SB}}} = \frac{2l_1 + l_2}{4l_1} = \frac{K_{11}}{2K_{22}}, \quad (24)$$

where we have used that $K_{11} = S^2(2l_1 + l_2)$ and $K_{22} = S^2(2l_1)$. From Eq. (24) and the overall minus signs in Eqs. (22) and (23), it is clear that at $S = S_c$, a second-order $N-N_{\text{TB}}$ occurs if $K_{11} > 2K_{22}$, while a second-order $N-N_{\text{SB}}$ occurs if $K_{11} < 2K_{22}$, in perfect agreement with the findings of Selinger and co-workers as well as of Dozov.^{3,6} As will be shown in Sec. VI, at S_c , the renormalized elastic constant K_{33}^{eff} vanishes, while K_{33} remains positive. A complete mapping of our LdG theory with the Oseen-Frank theory of Selinger follows. In particular, it can be observed that Eqs. (20)–(23) strongly resemble the expressions for the free-energy differences given in Refs. 6 and 7.

B. Phase transitions between spatially modulated nematic phases

The Oseen-Frank theories of Selinger and Dozov cannot describe phase transitions between periodically modulated nematic phases, since in these theories, the elastic constants do not explicitly depend on control parameters, in contrast with the LdG framework. However, for $l_3 = 0$ in the case of the LdG theory described in Subsection IV A, the elastic constants K_{11} , K_{22} , and K_{33} depend on S , but the ratio K_{11}/K_{22} is independent of S , and consequently, the theory predicts only either an $N-N_{\text{TB}}$ or an $N-N_{\text{SB}}$ phase transition. In order to overcome this limitation, we consider $l_3 \neq 0$ in Eq. (3). This procedure not only removes the degeneracy between K_{11} and K_{33}

but also allows the ratio K_{11}/K_{22} to vary with particle concentration. Extending the computation of Subsection IV A (for details, see the Appendix), we find that if $l_3 \neq 0$, the ratio of the (negative) grand potential densities of the N_{TB} and N_{SB} phases close to the transition point is given by

$$\begin{aligned} \frac{\Delta\Omega_{\text{TB}}}{\Delta\Omega_{\text{SB}}} &= \frac{2l_1 + l_2}{4l_1} + \frac{l_3}{8l_1} S \\ &= \frac{K_{11}}{2K_{22}} + \frac{3l_3}{8l_1} S, \end{aligned} \quad (25)$$

where we have used that $K_{11} = S^2(2l_1 + l_2 - Sl_3)$ and $K_{22} = S^2(2l_1)$. The critical scalar nematic order parameter at which $\Delta\Omega_{\text{TB}}$, $\Delta\Omega_{\text{SB}}$, and K_{33}^{eff} vanish reads

$$S_c = \frac{-4l_1 - 2l_2 + S_0 l_3}{2l_3} + \sqrt{\frac{-9S_0 \lambda^2}{4e_2 l_3} + \frac{(4l_1 + 2l_2 + S_0 l_3)^2}{4l_3^2}}. \quad (26)$$

From the linear S -dependence of Eq. (25), one can deduce that, depending on the values of l_1 , l_2 , and l_3 , either a second-order $N-N_{\text{TB}}$ phase transition occurs at S_c followed by a second-order $N_{\text{TB}}-N_{\text{SB}}$ phase transition at $S > S_c$ or a second-order $N-N_{\text{SB}}$ transition occurs at S_c succeeded by a second-order $N_{\text{SB}}-N_{\text{TB}}$ transition at $S > S_c$. To illustrate this, we map out the phase diagram as a function of the scalar nematic order parameter S and coefficient l_3 , for the coefficients $e_2 = 1$, $S_0 = 0.85$, $\kappa = 0.1L^2$, and $\lambda = 0.1L$. In Fig. 2, we display the resulting phase diagram three times with the background color denoting the values of the splay, twist, and bend elastic constants as indicated by the color bar. The $I-N$ transition occurs at a nematic order parameter value of $S_{IN} = 0.7922$. The green line in Fig. 2 corresponds to the set of points where the renormalized K_{33}^{eff} vanishes and hence the uniaxial N phase becomes unstable with respect to the spatially modulated phases. For $l_3 > -1.0L^2$ and $l_3 < -1.25L^2$, only a second-order $N-N_{\text{TB}}$ phase transition and a $N-N_{\text{SB}}$ phase transition occur, respectively, as a function of S . For $-1.25L^2 \leq l_3 \leq -1.0L^2$, instead, the $N-N_{\text{TB}}$ phase transition is followed by a second-order $N_{\text{TB}}-N_{\text{SB}}$ phase transition.

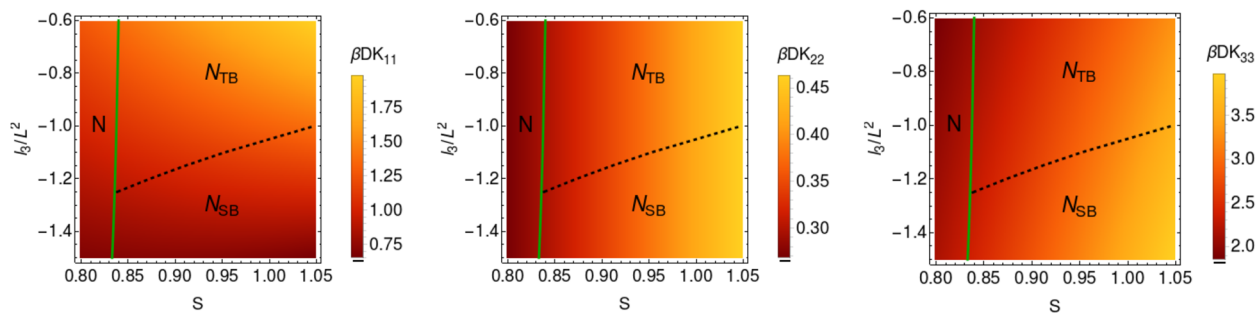


FIG. 2. Phase diagram as a function of the scalar nematic order parameter S and the coefficient l_3 for the coefficients $e_2 = 1$, $S_0 = 0.85$, $\kappa = 0.1L^2$, and $\lambda = 0.1L$, replicated three times with the background color denoting the value of the splay (K_{11}), twist (K_{22}), and bend (K_{33}) elastic constants as indicated by the color bar. The $I-N$ phase transition occurs at $S_{IN} = 0.7922$. The green line corresponds to the set of points where the renormalized bend elastic constant K_{33}^{eff} vanishes and hence the uniaxial N phase becomes unstable with respect to the spatially modulated nematic phases. For $l_3 > -1.0L^2$ and $l_3 < -1.25L^2$, only second-order $N-N_{\text{TB}}$ and $N-N_{\text{SB}}$ phase transitions occur as a function of S . For $-1.25L^2 < l_3 < -1.0L^2$, the $N-N_{\text{TB}}$ phase transition is followed by a second-order $N_{\text{TB}}-N_{\text{SB}}$ phase transition.

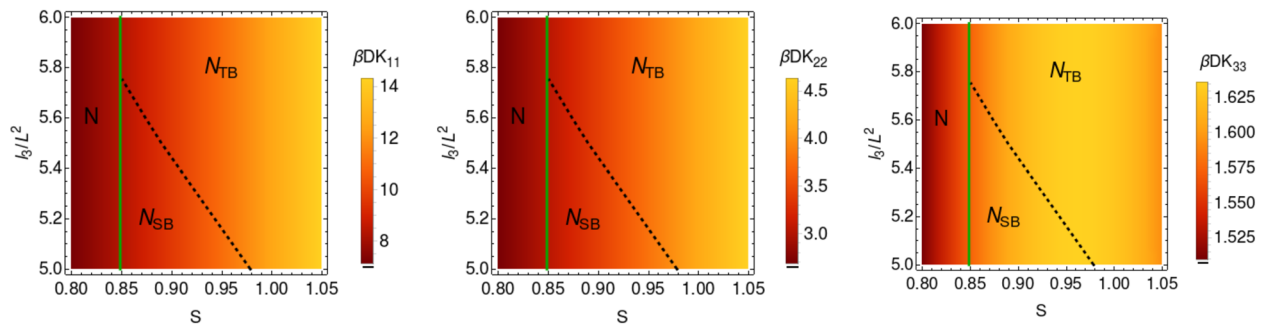


FIG. 3. Same as Fig. 2, but now for $l_1 = 1.65L^2$ and $l_2 = 0.854L^2$. For $l_3 < 5.75L^2$, the second-order N - N_{SB} transition is followed by a second-order N_{SB} - N_{TB} transition.

To map out the phase diagram of Fig. 2, we have used the coefficients $l_1 = 0.165L^2$ and $l_2 = 1.708L^2$, obtained from a fit to the results from Onsager theory of hard rods, as stated in Sec. III. For a different choice, $l_1 = 1.65L^2$ and $l_2 = 0.854L^2$, the phase sequence of N - N_{TB} - N_{SB} can be replaced by a N - N_{SB} - N_{TB} phase sequence, as shown in Fig. 3. Again, the I - N phase transition occurs at $S_{IN} = 0.7922$, the green line corresponds to the set of points where the uniaxial N phase becomes unstable with respect to the spatially modulated phases, and the background color denotes the values of K_{11} , K_{22} , and K_{33} . We clearly observe from Fig. 3 that for $l_3 < 5.75L^2$, the second-order N - N_{SB} phase transition is followed by a second-order N_{SB} - N_{TB} transition.

V. FIRST-ORDER N - N_{TB} PHASE TRANSITION

We now consider the LdG theory of Sec. II with $e_6 > 0$ and allow e_4 to change sign in order to describe the first-order N - N_{TB} phase transition recently found in Onsager theory and simulations.^{19,36} For the sake of simplicity, we set $l_3 = 0$ corresponding to a degenerate splay and bend elastic constant. We again start by inserting the nematic director $\hat{n}_{TB}(z)$ into the nematic tensor order parameter [Eq. (4)] and by inserting the resulting $\mathbf{Q}(z)$ together with $\mathbf{P}_{TB}(z)$ in the grand potential [Eq. (1)]. Minimizing the obtained grand potential with respect to the wave number q and the tilt angle θ , we find expressions (12) and (13) already found in Sec. IV. We perform a stability analysis inserting these expressions into the grand potential [Eq. (1)] and minimize the resulting Ω with respect to S and P at fixed μ , i.e., we solve the Euler-Lagrange equations $\partial\Delta\Omega/\partial S = 0$ and $\partial\Delta\Omega/\partial P = 0$. Analytically solving this system is cumbersome since the two equations take the form of polynomials of third and fifth orders, respectively, with a nonzero constant term. For this reason, we directly minimize the grand potential Ω using a simulated annealing algorithm.⁵² In this way, we obtain S and P as a function of μ . Note that in contrast to the situation discussed in Sec. IV, we cannot perform a stability analysis by minimizing Ω with respect to P at fixed S , i.e., by solving the Euler-Lagrange equation $\partial\Delta\Omega/\partial P = 0$. A jump in S is expected at a first-order N - N_{TB} phase transition, and while we know the expression of S_N as a function of μ , we do not know $S_{N_{TB}}$ as a function of μ analytically. Nevertheless, valuable insight can yet be obtained from the expression for P as a function of S . For example, expressions can be derived for the spinodal of the

uniaxial N phase with respect to N_{TB} and for the spinodal of the N_{TB} phase with respect to the uniaxial N phase. Hence, the limits of stability of the N and N_{TB} phases are analytically known. For small P , the solutions of the Euler-Lagrange equation $\partial\Delta\Omega/\partial P = 0$ are given by

$$\begin{aligned} P_0(S) &= 0, \\ P_1^\pm(S) &= \pm \sqrt{\frac{-16e_4 - \sqrt{\gamma(S)}}{48e_6}}, \\ P_2^\pm(S) &= \pm \sqrt{\frac{-16e_4 + \sqrt{\gamma(S)}}{48e_6}}, \end{aligned} \quad (27)$$

with $\gamma(S) = 256e_4^2 - 96e_6(8e_2 - 8Se_2/S_0 - 9\lambda^2/(2l_1 + l_2))$. The solution $P_0(S)$ corresponds to the uniaxial N phase. If $e_4 < 0$, we find for an increase in S , a jump from the uniaxial N phase corresponding to $P_0(S)$ to the two (equivalent) solutions $P_2^\pm(S)$, while the solutions $P_1^\pm(S)$ are always metastable. The solutions $P_2^\pm(S)$ represent the N_{TB} phase with the equilibrium wave vector q and equilibrium angle θ given by Eqs. (12) and (13), respectively. The spinodal of the N_{TB} phase with respect to the uniaxial N phase, given by the condition $\partial^2\Delta\Omega/\partial^2P|_{P=P_2^\pm} = 0$, is at

$$S^+ = S_0 \left(1 - \frac{9\lambda^2}{8e_2(2l_1 + l_2)} - \frac{e_4^2}{4e_2e_6} \right), \quad (28)$$

while the spinodal of the uniaxial N phase with respect to the N_{TB} phase, given by the condition $\partial^2\Delta\Omega/\partial^2P|_{P=P_0} = 0$, is at

$$S^* = S_0 \left(1 - \frac{9\lambda^2}{8e_2(2l_1 + l_2)} \right). \quad (29)$$

If instead $e_4 \geq 0$, we find a second-order phase transition from the N phase with $P_0(S) = 0$ to the N_{TB} phase with $P_2^\pm(S)$ at $S_c = S_0(1 - 9\lambda^2/(8e_2(2l_1 + l_2)))$, while the solutions $P_1^\pm(S)$ are imaginary and hence unphysical. Note that the nematic spinodal of the first-order N - N_{TB} phase transition coincides with the transition point of the second-order N - N_{TB} transition. Furthermore, the transition point of the second-order N - N_{TB} transition found in this section coincides with the one found in Sec. IV.

Exemplarily, we show the analytical solutions for the amplitude of the polar vector P (27) and the equilibrium wave vector q denoted

in orange and tilt angle θ denoted in violet as given by Eqs. (12) and (13) in Fig. 4 as a function of the scalar nematic order parameter S for the coefficients $e_2 = 1$, $S_0 = 0.85$, $\lambda = 0.08L$, $\kappa = 0.1L^2$, $e_6 = 10$, and $e_4 = -1$ [Fig. 4(a)] and $e_4 = 1$ [Fig. 4(b)]. The uniaxial N solution $P_0(S) = 0$ is represented by a red full line when it is stable and by a red dashed line when it is metastable. The N_{TB} solution $P_2^\pm(S)$ is represented by a black full line, while the metastable solutions $P_1^\pm(S)$ are represented by black dashed lines. We find that in (a), the spinodal of the N_{TB} phase with respect to the uniaxial N phase is at

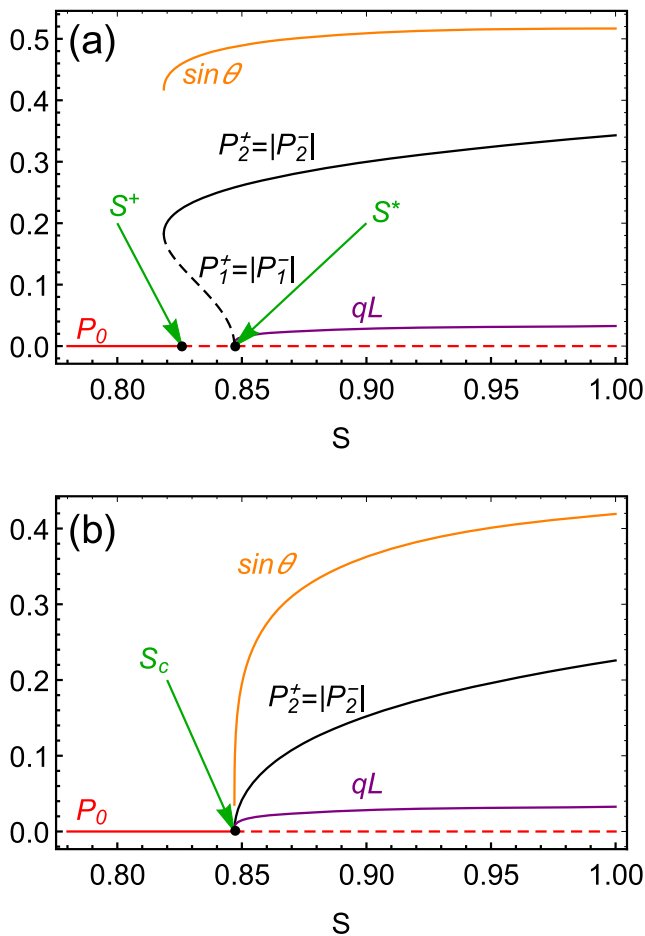


FIG. 4. Amplitude of the polar vector P and the equilibrium wave number q , and tilt angle θ as given by Eqs. (27), (12), and (13), respectively, as a function of the scalar order parameter S for the coefficients $e_2 = 1$, $S_0 = 0.85$, $\lambda = 0.08L$, $\kappa = 0.1L^2$, $e_6 = 10$, and $e_4 = -1$ (a) or $e_4 = 1$ (b). The uniaxial N solution $P_0(S) = 0$ is represented by a red full line when it is stable and by a red dashed line when it is metastable. The N_{TB} solution $P_2^\pm(S)$ is represented by a black full line, while the metastable solutions $P_1^\pm(S)$ are represented by black dashed lines. The equilibrium q and θ are represented in orange and violet, respectively. In (a), the spinodal of the N_{TB} phase with respect to the uniaxial N phase is at $S^+ = 0.826$, while the spinodal of the uniaxial N phase with respect to the N_{TB} phase is at $S^* = 0.847$. In (b), the second-order $N-N_{TB}$ transition occurs at $S_c = 0.847$. We observe that $S^* = S_c$, i.e., the nematic spinodal of a first-order $N-N_{TB}$ phase transition becomes the transition point if the $N-N_{TB}$ transition is second-order.

$S^+ = 0.826$, while the spinodal of the uniaxial N phase with respect to the N_{TB} phase is at $S^* = 0.847$. In (b), the second-order $N-N_{TB}$ transition occurs at $S_c = 0.847$. We note that $S^* = S_c$, i.e., the nematic spinodal of a first-order $N-N_{TB}$ phase transition becomes the transition point if the $N-N_{TB}$ transition is second-order. In addition, we find that in the case of a second-order $N-N_{TB}$ phase transition, the equilibrium q and θ tend to zero at the transition, in agreement with Refs. 6 and 20.

The solutions $S(\mu)$ and $P(\mu)$ as obtained by directly minimizing Ω are plotted in Fig. 5. In addition, we plot θ , q , and $S \cos \theta$ as a function of μ . The dependence on chemical potential in Fig. 5 is then converted to concentration in Fig. 6. If $e_4 = -1$, upon increasing μ , we find the “Onsager”-type first-order $I-N$ phase transition described

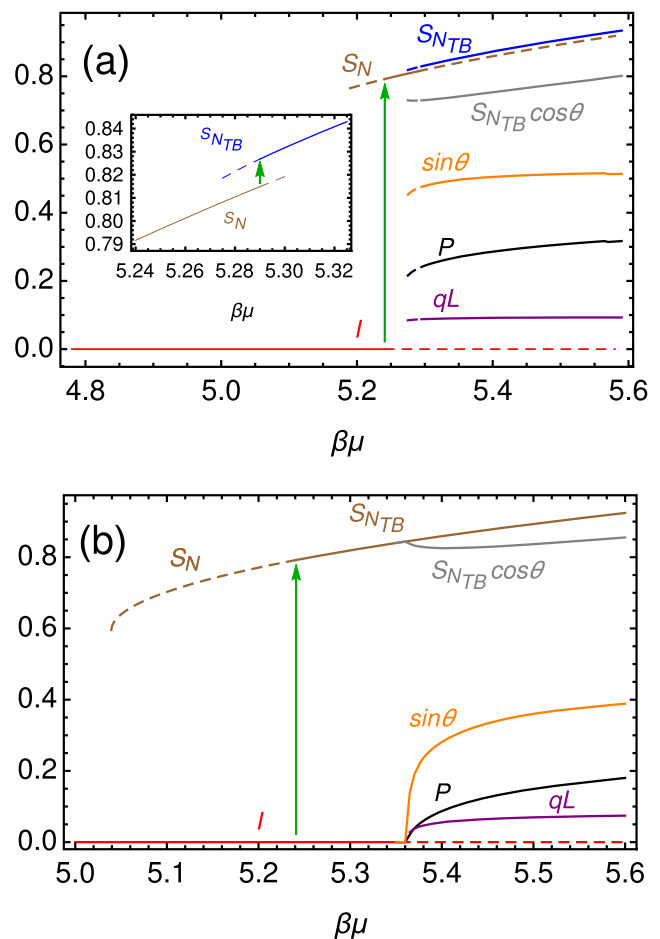


FIG. 5. Scalar nematic order parameter (brown and blue) and amplitude of the polarity P (black) as a function of the chemical potential $\beta\mu$ for the coefficients $e_2 = 1$, $\lambda = 0.08L$, $\kappa = 0.1L^2$, $e_6 = 10$, $S_0 = 0.85$, and $e_4 = -1$ (a) or $e_4 = 1$ (b). The equilibrium q and θ are represented in orange and violet, respectively. In (a), the “Onsager”-type first-order $I-N$ transition at $\beta\mu_{IN} = 5.241$ is followed by a weakly first-order $N-N_{TB}$ transition at $\beta\mu_{NN_{TB}} = 5.293$. In (b), the “Onsager”-type first-order $I-N$ transition is instead followed by a continuous second-order $N-N_{TB}$ transition at $\beta\mu_{NN_{TB}} = 5.36$.

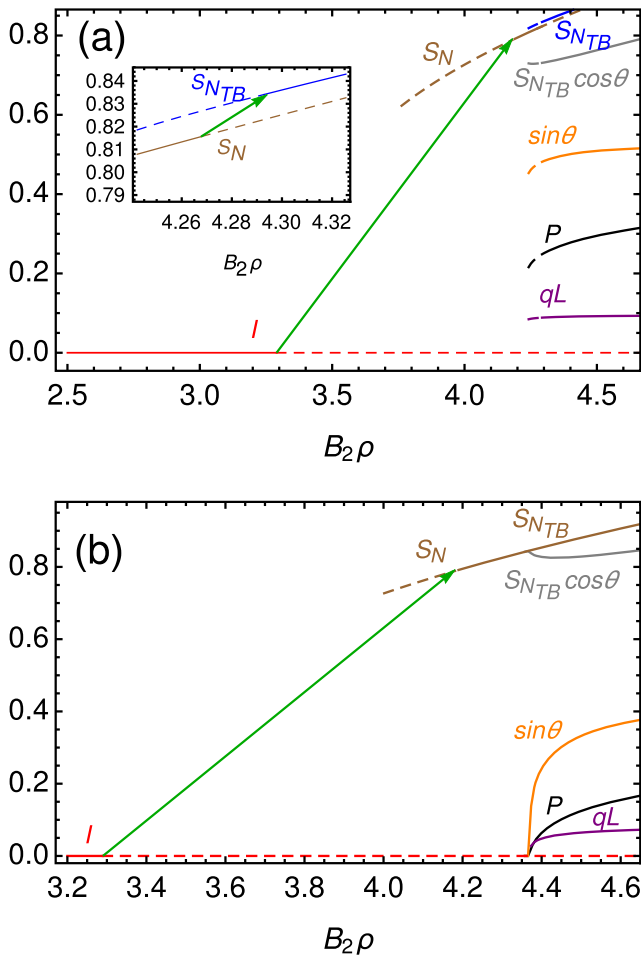


FIG. 6. Scalar nematic order parameter (brown and blue) and amplitude of the polarity P (black) as a function of the particle concentration $c = B_2\rho$ for the coefficients $e_2 = 1$, $\lambda = 0.08L$, $\kappa = 0.1L^2$, $e_6 = 10$, $S_0 = 0.85$, and $e_4 = -1$ (a) or $e_4 = 1$ (b). The equilibrium q and θ are represented in orange and violet, respectively. In (a), the “Onsager”-type first-order I - N transition with coexisting concentrations $c_I = 3.290$ and $c_N = 4.191$ is followed by a weakly first-order N - N_{TB} transition with coexisting concentrations $c_N = 4.265$ and $c_{N_{TB}} = 4.295$, i.e., a density jump on the order of 1%. The inset shows a zoomed-in view of the discontinuous jump in the scalar order parameter at the N - N_{TB} transition. In (b), the “Onsager”-type first-order I - N transition is instead followed by a continuous second-order N - N_{TB} transition at $c_N = c_{N_{TB}} = 4.36$.

in Sec. III, followed by a weakly first-order N - N_{TB} phase transition at $\beta\mu_{NN_{TB}} = 5.293$, where the nematic order parameter jumps from $S_N = 0.814$ to $S_{N_{TB}} = 0.836$. The coexisting densities are $c_N = 4.265$ and $c_{N_{TB}} = 4.295$, i.e., a density jump on the order of 1%. Interestingly, we also find jumps in P , θ , q , and $S_N \cos \theta$, which is to be contrasted with a second-order N - N_{TB} phase transition. For instance, upon increasing the chemical potential μ for the parameter $e_4 = 1$, we find an “Onsager”-type I - N phase transition and subsequently a second-order N - N_{TB} transition at $\beta\mu_{NN_{TB}} = 5.36$, where $S_N(\mu_{NN_{TB}}) = S_{N_{TB}}(\mu_{NN_{TB}}) = 0.847$, $c_N = c_{N_{TB}} = 4.36$, and $P = \theta = q = 0$, so no jumps at all.

Finally, we map out two phase diagrams of Figs. 7(a) and 7(b). In Fig. 7(a), we plot the phase diagram as a function of the particle concentration $c = B_2\rho$ and the modulus of the flexoelectric coupling coefficient $|\lambda|$ for the same coefficients as above, i.e., $e_2 = 1$, $S_0 = 0.85$, $e_4 = -1$, $\kappa = 0.1L^2$, and $e_6 = 10$. The pink regions represent two-phase coexistence regions. At $|\lambda| < 0.14L$, the phase diagram features the “Onsager”-type first-order I - N transition followed by a weakly first-order N - N_{TB} transition at higher densities. At $|\lambda| > 0.14L$, however, we find a direct first-order I - N_{TB} transition of which the coexisting densities decrease with an increase in $|\lambda|$. The two regimes are separated by an I - N - N_{TB} triple point at $|\lambda| = 0.14L$. It is important to observe that the I - N_{TB} transition remains always first-order such that we never find a second-order I - N_{TB} transition. Moreover, at $\lambda = 0$, a first-order phase transition is found from a uniaxial N phase to an N_{TB} phase with an infinite pitch, i.e., a polar nematic phase. In Fig. 7(b), instead, we build a phase diagram as a function of particle concentration $c = B_2\rho$ and coefficient e_4 of the $|P|^4$ term that we allow to be negative because of the presence of a stabilizing (positive) $|P|^6$ term in the grand potential. We fix the other coefficients to the values as employed above, i.e., $e_2 = 1$, $\lambda = 0.08L$, $\kappa = 0.1L^2$, $e_6 = 10$, and $S_0 = 0.85$. Again, the pink regions represent bulk coexistence regions. We note that we have chosen a value of λ such that the I - N transition is followed by an N - N_{TB} transition at $e_4 = -1$ according to Fig. 7(a). For $-1.5 < e_4 < 0$, we find the “Onsager”-type first-order I - N transition followed by a weakly first-order N - N_{TB} transition. We observe, however, a direct strongly first-order I - N_{TB} transition for $e_4 < -1.5$ and an I - N - N_{TB} triple point at $e_4 = -1.5$. Furthermore, we find that the line of first-order N - N_{TB} transitions ends in a tricritical point at $(c = 4.3, e_4 = 0)$. At $e_4 > 0$, the N - N_{TB} transition ceases to be first-order and becomes second-order as illustrated by the dashed line.

As a final observation, we mention that the formalism introduced in this section should also hold for the N_{SB} phase. Despite reasonable efforts, but not exhaustive, we did not find a set of coefficients for which the N_{SB} phase is more stable than the N_{TB} one. However, since in simulations and Onsager theory only an N - N_{TB} phase transition was found, we focused on the latter one. Very interestingly, the nematic spinodal of such a putative N - N_{SB} transition would coincide with the nematic spinodal of the N - N_{TB} phase found here. Furthermore, by breaking the degeneracy between K_{11} and K_{33} , i.e., by setting $l_3 \neq 0$ in Eq. (3), the first-order N - N_{TB} phase transition described in this section could be followed by a first-order N_{TB} - N_{SB} phase transition.

VI. RENORMALIZED ELASTIC CONSTANTS

The flexoelectric coupling term $-\lambda P_\alpha \partial_\beta Q_{\beta\alpha}$ of Eq. (6) affects the elastic response of polar nematic phases, which translates into renormalized elastic constants. In order to quantify the renormalization of the elastic constants, we follow the procedure of Refs. 1 and 6. First, we solve the Euler-Lagrange equation $\partial(\beta B_2 \omega_P)/\partial P_\rho = 0$. By using Eq. (4) for the tensor order parameter \mathbf{Q} , the fact that \mathbf{P} and $\hat{\mathbf{n}}$ are perpendicular, i.e., $P_\alpha n_\alpha = 0$, and the fact that $P_\alpha P_\alpha = 0$ in the uniaxial N phase, we find

$$P_\rho = \frac{\lambda S_0}{2e_2(S_0 - S)} \partial_\gamma Q_{\rho\gamma}, \quad (30)$$

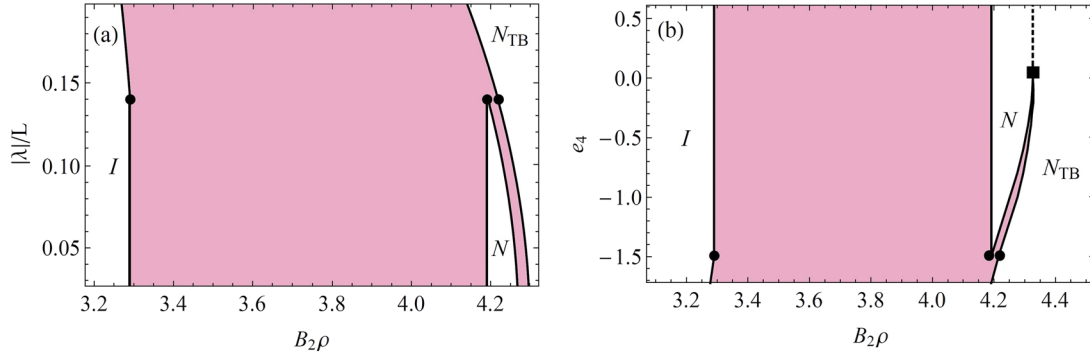


FIG. 7. (a) Phase diagram as a function of the particle concentration $c = B_2\rho$ and the modulus of the flexoelectric coupling coefficient $|\lambda|/L$ for the coefficients $e_2 = 1$, $S_0 = 0.85$, $e_4 = -1$, $\kappa = 0.1L^2$, and $e_6 = 10$. For a weak flexoelectric coupling ($|\lambda| < 0.14L$), an “Onsager”-type first-order $I-N$ transition is followed by a weakly first-order $N-N_{TB}$ transition, while for strong coupling ($|\lambda| > 0.14L$), a direct strongly first-order $I-N_{TB}$ transition occurs. A $I-N-N_{TB}$ triple point stabilizes at $|\lambda| = 0.14L$. (b) Phase diagram as a function of the particle concentration $c = B_2\rho$ and the coefficient e_4 for the coefficients $e_2 = 1$, $\lambda = 0.08L$, $\kappa = 0.1L^2$, $e_6 = 10$, and $S_0 = 0.85$. For $-1.5 < e_4 < 0$, the “Onsager”-type first-order $I-N$ transition is followed by a weakly first-order $N-N_{TB}$ phase transition, while a strongly first-order $I-N_{TB}$ transition occurs for $e_4 < -1.5$. A $I-N-N_{TB}$ triple point stabilizes at $e_4 = -1.5$. The line of first-order $N-N_{TB}$ transitions ends in a tricritical point ($c = 4.3$, $e_4 = 0$), from where it continues as a second-order $N-N_{TB}$ transition. In (a) and (b), the circles indicate triple points, the square indicates the tricritical point, the pink regions represent coexistence regions, and the dashed line indicates a second-order transition.

which upon insertion into Eq. (6), with $l_3 = 0$ for convenience, yields

$$\begin{aligned} \beta B_2 \omega_P = & -\frac{\lambda^2 S_0 (S_0 - 2S)}{4e_2 (S_0 - S)^2} (\partial_\gamma Q_{\gamma\alpha}) (\partial_\beta Q_{\beta\alpha}) \\ & + \frac{\lambda^2 S_0}{2e_2 (S_0 - S)^2} (\partial_\gamma Q_{\gamma\alpha}) Q_{\alpha\beta} (\partial_\xi Q_{\xi\beta}). \end{aligned} \quad (31)$$

In the final step, we neglected the terms $e_4 P_\alpha P_\alpha P_\beta P_\beta$, $\kappa (\partial_\alpha P_\beta) (\partial_\alpha P_\beta)$ and $e_6 P_\alpha P_\alpha P_\beta P_\beta P_\gamma P_\gamma$ in Eq. (6) because they do not contribute to the linear elasticity as they contain derivatives of the nematic director of order higher than two. It follows that the form of the renormalized elastic constant is the same for second-order transitions ($e_4 > 0$, $e_6 \geq 0$) as well as for first-order ones ($e_4 < 0$, $e_6 > 0$). Using that $n_i (\partial_j n_i) = (\partial_j n_i) n_i = 0$ and that

$$\begin{aligned} (\partial_\alpha n_\beta) (\partial_\alpha n_\beta) = & (\nabla \cdot \hat{\mathbf{n}})^2 + [\hat{\mathbf{n}} \cdot (\nabla \times \hat{\mathbf{n}})]^2 + |\hat{\mathbf{n}} \times (\nabla \times \hat{\mathbf{n}})|^2 \\ & - \nabla \cdot [\hat{\mathbf{n}} (\nabla \cdot \hat{\mathbf{n}}) + \hat{\mathbf{n}} \times (\nabla \times \hat{\mathbf{n}})], \end{aligned} \quad (32)$$

we find

$$\begin{aligned} \beta B_2 (\omega_e + \omega_P) = & \left[l_1 + \frac{1}{2} l_2 - \frac{S_0 - 4S}{S_0 - S} \xi(S) \right] S^2 (\nabla \cdot \hat{\mathbf{n}})^2 \\ & + \left[l_1 + \frac{1}{2} l_2 - \xi(S) \right] S^2 |\hat{\mathbf{n}} \times (\nabla \times \hat{\mathbf{n}})|^2 \\ & + \frac{1}{3} \left[2l_2 + \frac{10S - 3S_0}{S_0 - S} \xi(S) \right] S (\nabla \cdot \hat{\mathbf{n}}) (\nabla S \cdot \hat{\mathbf{n}}) \\ & + \left[\frac{1}{6} l_2 - \frac{S_0 - 3S}{S_0 - S} \xi(S) \right] (\nabla S \cdot \hat{\mathbf{n}})^2 + \left[\frac{1}{3} l_2 - \xi(S) \right] |\nabla S|^2 \\ & + l_1 S^2 \{ [\hat{\mathbf{n}} \cdot (\nabla \times \hat{\mathbf{n}})]^2 - \nabla \cdot [\hat{\mathbf{n}} (\nabla \cdot \hat{\mathbf{n}}) + \hat{\mathbf{n}} \times (\nabla \times \hat{\mathbf{n}})] \}, \end{aligned} \quad (33)$$

with $\xi(S) = 9\lambda^2 S_0 / (16e_2 (S_0 - S))$. Comparing Eq. (33) with the Oseen–Frank elastic energy (5) gives us the renormalized splay

(K_{11}^{eff}), twist (K_{22}^{eff}), and bend (K_{33}^{eff}) elastic constants

$$\begin{aligned} \beta DK_{11}^{\text{eff}} = & \beta DK_{11} - \frac{8S^2}{\pi L^2} \frac{S_0 - 4S}{S_0 - S} \xi(S), \\ \beta DK_{22}^{\text{eff}} = & \beta DK_{22}, \\ \beta DK_{33}^{\text{eff}} = & \beta DK_{33} - \frac{8S^2}{\pi L^2} \xi(S), \end{aligned} \quad (34)$$

where K_{11} , K_{22} , and K_{33} are the bare splay, twist, and bend elastic constants discussed in Sec. II. Equation (34) directly reveals the flexoelectric coupling as the source of the renormalization, since $\lambda = 0$ gives $\xi(S) = 0$ and hence no renormalization at all. For $\lambda \neq 0$, we observe, however, that the renormalization procedure breaks the degeneracy between the renormalized splay and bend elastic constants, so even though $K_{11} = K_{33}$, we have nevertheless that $K_{11}^{\text{eff}} \neq K_{33}^{\text{eff}}$. The renormalization does not affect the twist elastic constant, for which $K_{22} = K_{22}^{\text{eff}}$. The elastic constants K_{11}^{eff} , $K_{22}^{\text{eff}} = K_{22}$ and $K_{11} = K_{33}$ increase monotonically with S , while the renormalized bend elastic constant K_{33}^{eff} starts to decrease beyond a certain value of S until it becomes zero at $S_c = S_0 (1 - 9\lambda^2 / (8e_2 (2l_1 + l_2)))$. As discussed in Secs. IV and V, the second-order $N-N_{TB}$ phase transition occurs at a nematic order parameter value S_c , whereas in the case of a first-order transition, the spinodal of the N phase with respect to the N_{SB} phase is located at S_c . As a consequence, our result is in agreement with Selinger’s one in the case of a second-order $N-N_{TB}$ transition, while in the case of a first-order transition, we find that at the transition point, both $K_{33} > 0$ and $K_{33}^{\text{eff}} > 0$. In the latter case, K_{33}^{eff} becomes zero at the nematic spinodal. The bare and the renormalized elastic constants are plotted as a function of the scalar order parameter S in Fig. 8 for the coefficients $e_2 = 1$, $S_0 = 1$, $\lambda = 0.08L$, and $e_6 = 10$. The monotonic increase in K_{11}^{eff} , $K_{22}^{\text{eff}} = K_{22}$ and $K_{11} = K_{33}$ with S , together with the simultaneous softening of K_{33}^{eff} , can be observed in Fig. 8. The picture is qualitatively the same for $l_3 \neq 0$, with K_{33}^{eff} vanishing at S_c as given by Eq. (26).

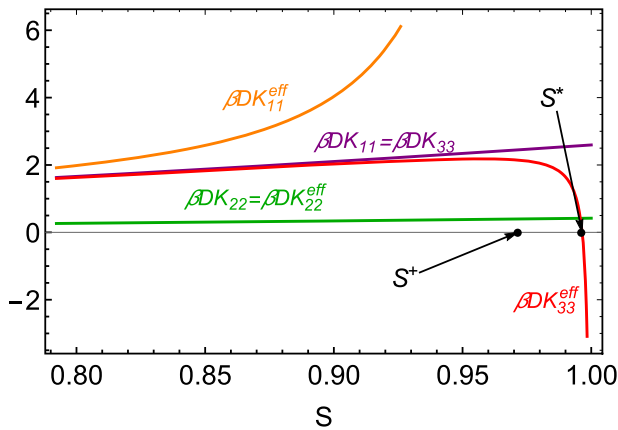


FIG. 8. Bare (K_{11}, K_{22}, K_{33}) and renormalized ($K_{11}^{\text{eff}}, K_{22}^{\text{eff}}, K_{33}^{\text{eff}}$) splay, twist, and bend elastic constants as a function of the scalar nematic order parameter S for the fixed values of the coefficients $e_2 = 1$, $S_0 = 1$, $\lambda = 0.08L$, and $e_6 = 10$. While $K_{11}^{\text{eff}}, K_{11} = K_{33}$, and $K_{22}^{\text{eff}} = K_{22}$ increase monotonically with S , K_{33}^{eff} starts to decrease beyond a certain value of S , until it becomes zero at $S = S_0(1 - 9\lambda^2/(8e_2(2l_1 + l_2)))$. This nematic order parameter value S_c is where the $N-N_{\text{TB}}$ transition occurs if it is second-order, while it is the spinodal S^* of the N phase with respect to the N_{TB} one in the case of a first-order $N-N_{\text{TB}}$ transition. S^+ indicates the spinodal of the N_{TB} phase with respect to the uniaxial N one.

VII. CONCLUSIONS AND DISCUSSION

In this paper, we have developed a phenomenological LdG theory for lyotropic suspensions of bent hard rods, using a Q -tensor expansion of the chemical-potential dependent grand potential. In addition, we introduce a bend flexoelectric term that couples the polarization and the divergence of the Q -tensor to study the stability of uniaxial (N), twist-bend (N_{TB}), and splay-bend (N_{SB}) nematic phases of colloidal bent rods as a function of particle concentration. We first showed that our LdG theory can be mapped onto an Oseen-Frank theory. Subsequently, by breaking the degeneracy between the splay and bend elastic constants, we find that the LdG theory predicts either an $N-N_{\text{TB}}-N_{\text{SB}}$ or an $N-N_{\text{SB}}-N_{\text{TB}}$ phase sequence upon increasing the particle concentration. We have mapped out several phase diagrams as a function of the particle concentration

that can be used as guidelines for experiments, simulations, and microscopic theories. In addition, we have focused on the first-order $N-N_{\text{TB}}$ phase transition. Our model is able to reproduce the discontinuous jumps associated with this transition, including the density jump and the discontinuities in the polarization and nematic order. Moreover, in contrast to the case of a second-order $N-N_{\text{TB}}$ phase transition where the bend elastic constant K_{33} is positive while its renormalized version K_{33}^{eff} vanishes, we have found that K_{33}^{eff} vanishes at the nematic spinodal in the case of a first-order $N-N_{\text{TB}}$ transition so that K_{33} and K_{33}^{eff} remain positive at the actual transition point. This finding appears to be general and could help in understanding the problem of the softening of the elastic constants in systems with spontaneous polar order and of the mechanism driving the onset of the spatially modulated phases in bent-core liquid crystals.

Finally, it is interesting to employ the LdG theory to study confinement effects of these spatially modulated nematic phases and to investigate the structure of the interface between a coexisting N_{TB} and an N_{SB} phase with either an isotropic, uniaxial nematic or a substrate. We will postpone this to future work.

ACKNOWLEDGMENTS

The authors acknowledge help by S. Paliwal with the numerical calculations and by A. Grau Carbonell in the realization of Fig. 1. They acknowledge financial support from the “Nederlandse Organisatie voor Wetenschappelijk Onderzoek” (NWO) TOPPUNT. This work was part of the D-ITP consortium, a program of the NWO that is funded by the Dutch Ministry of Education, Culture and Science (OCW).

APPENDIX: GRAND POTENTIAL DENSITY OF THE N_{TB} AND N_{SB} PHASES FOR $l_3 \neq 0$.

In order to compute the grand potential density of the N_{TB} phase, we insert $\hat{\mathbf{n}}_{\text{TB}} = (\sin \theta \cos(qz), \sin \theta \sin(qz), \cos \theta)$ in the tensor order parameter $Q_{\alpha\beta}(\mathbf{r}) = \frac{3}{2}S(\mathbf{r})(n_\alpha(\mathbf{r})n_\beta(\mathbf{r}) - \frac{1}{3}\delta_{\alpha\beta})$ and the resulting \mathbf{Q} , together with $\mathbf{P}_{\text{TB}} = (P \sin(qz), -P \cos(qz), 0)$, in the grand potential given by Eq. (1). We minimize the obtained grand potential with respect to the wave number q and the tilt angle θ , respectively, and find

$$q_{\text{TB}} = \frac{3\lambda \sin(2\theta_{\text{TB}})SP}{8\kappa P^2 + 4S^2(2l_1 + l_2) \sin^2 \theta_{\text{TB}} - 4l_2 S^2 \sin^4 \theta_{\text{TB}} + 2S^3 l_3 (\sin^2 \theta_{\text{TB}} - \sin^4 \theta_{\text{TB}})} \quad (\text{A1})$$

and

$$\sin^2 \theta_{\text{TB}} = \frac{\kappa P^2}{S^2 l_1} + \frac{\sqrt{\kappa P^2 (\kappa P^2 + S^2 l_1)}}{S^2 l_1}. \quad (\text{A2})$$

Inserting (A1) and (A2) back into Eq. (1), and approximating for small P , the grand potential density in the N_{TB} phase is given by

$$\begin{aligned} \frac{\Delta\Omega_{TB}}{V} &= \frac{\Delta\Omega}{V} - \frac{\Delta\Omega_N}{V} \\ &= \left[\frac{e_2(S_0 - S)}{S_0} - \frac{9\lambda^2}{4(4l_1 + 2l_2 + Sl_3)} \right] P^2 \\ &\quad + \frac{18\lambda^2 \sqrt{\kappa S^2 I_1}}{S^2(4l_1 + 2l_2 + Sl_3)^2} |P|^3 + e_4 P^4 + O(P^5), \end{aligned} \quad (A3)$$

where $\Delta\Omega_N/V = aS^2(\mu^* - \mu) - bS^3 + dS^4$ is the grand-potential density of the N phase.

Analogously, in order to compute the grand potential density of the N_{SB} phase, we insert the nematic director $\hat{n}_{SB} = (\sin(\theta \sin(qz)), 0, \cos(\theta \sin(qz)))$ into the tensor order parameter $Q_{\alpha\beta}(\mathbf{r}) = \frac{3}{2}S(\mathbf{r})(n_\alpha(\mathbf{r})n_\beta(\mathbf{r}) - \frac{1}{3}\delta_{\alpha\beta})$ and the resulting \mathbf{Q} , together with $\mathbf{P}_{SB} = (-P \cos(qz) \cos(\theta \sin(qz)), 0, \frac{1}{2}P \cos(qz) \sin(2\theta \sin(qz)))$, into the grand potential given by Eq. (1) and average it over a full period $2\pi/q$. We then minimize the obtained grand potential with respect to the wave number q and the tilt angle θ , respectively, and find

$$q_{SB} = \frac{3\lambda\theta_{SB}(\theta_{SB}^2 - 8)PS}{8(4 + 3\theta_{SB}^2)\kappa P^2 + 16S^2(2l_1 + l_2 + Sl_3)\theta_{SB}^2} \quad (A4)$$

and

$$\theta_{SB}^2 = \frac{16\kappa P^2}{3\kappa P^2 + \sqrt{\kappa P^2(57\kappa P^2 + 16S^2(4l_1 + 2l_2 + Sl_3))}}. \quad (A5)$$

Inserting Eqs. (A4) and (A5) back into Eq. (1) and approximating for small P , the grand potential density of the N_{SB} phase reads

$$\begin{aligned} \frac{\Delta\Omega_{SB}}{V} &= \frac{\Delta\Omega}{V} - \frac{\Delta\Omega_N}{V} \\ &= \left[\frac{e_2(S_0 - S)}{2S_0} - \frac{9\lambda^2}{8(4l_1 + 2l_2 + Sl_3)} \right] P^2 \\ &\quad - \frac{9\lambda^2 \sqrt{\kappa S^2(4l_1 + 2l_2 + Sl_3)}}{4S^2(4l_1 + 2l_2 + Sl_3)^2} |P|^3 + \frac{3}{8}e_4 P^4 + O(P^5), \end{aligned} \quad (A6)$$

where $\Delta\Omega_N/V = aS^2(\mu^* - \mu) - bS^3 + dS^4$ is again the grand potential density of the N phase.

We observe that for small P , both $\Delta\Omega_{TB}$ and $\Delta\Omega_{SB}$ vanish at the critical point S_c given by Eq. (26). Close to this point, we can assume $P_{TB} \ll 18\lambda^2 \sqrt{\kappa S^2 I_1} / (e_4 S^2(4l_1 + 2l_2 + Sl_3)^2)$ and $P_{SB} \ll 6\lambda^2 \sqrt{\kappa S^2(4l_1 + 2l_2 + Sl_3)} / (e_4 S^2(4l_1 + 2l_2 + Sl_3)^2)$ such that the cubic terms dominate over the quartic terms in Eqs. (A3) and (A6). Solving the Euler-Lagrange equations $\partial(\Delta\Omega_{TB}/V)/\partial P = 0$ and $\partial(\Delta\Omega_{SB}/V)/\partial P = 0$, we find

$$P_{TB} = \frac{(9\lambda^2 S_0 - 4e_2(S_0 - S)(4l_1 + 2l_2 + Sl_3))(4l_1 + 2l_2 + Sl_3)S^2}{108\lambda^2 I_1 S_0 \sqrt{\kappa S^2 I_1}} \quad (A7)$$

and

$$P_{SB} = \frac{(9\lambda^2 S_0 - 4e_2(S_0 - S)(4l_1 + 2l_2 + Sl_3))\sqrt{\kappa S^2(4l_1 + 2l_2 + Sl_3)}}{27\lambda^2 \kappa S_0}, \quad (A8)$$

respectively. Inserting these back in Eqs. (A3) and (A6) gives close to the transition

$$\frac{\Delta\Omega_{TB}}{V} = \frac{(-9\lambda^2 S_0 + 4e_2(S_0 - S)(4l_1 + 2l_2 + Sl_3))^3 (4l_1 + 2l_2 + Sl_3)S^2}{46\,656\kappa\lambda^2 I_1 S_0^3} \quad (A9)$$

and

$$\frac{\Delta\Omega_{SB}}{V} = \frac{(-9\lambda^2 S_0 + 4e_2(S_0 - S)(4l_1 + 2l_2 + Sl_3))^3 S^2}{5832\kappa\lambda^2 S_0^3}, \quad (A10)$$

respectively. The ratio between the grand potential densities (A9) and (A10) is then given by Eq. (25).

DATA AVAILABILITY

The data that support the findings of this study are available from the corresponding author upon reasonable request.

REFERENCES

- A. Jáklí, O. D. Lavrentovich, and J. V. Selinger, "Physics of liquid crystals of bent-shaped molecules," *Rev. Mod. Phys.* **90**, 045004 (2018).
- R. B. Meyer, "Piezoelectric effects in liquid crystals," *Phys. Rev. Lett.* **22**, 918–921 (1969).
- I. Dozov, "On the spontaneous symmetry breaking in the mesophases of achiral banana-shaped molecules," *Europhys. Lett.* **56**, 247–253 (2001).
- R. B. Meyer, "Structural problems in liquid crystal physics," in *Molecular Fluids*, Les Houches Summer School in Theoretical Physics, edited by R. Balian and G. Weill (Gordon & Breach, New York, 1976), pp. 271–343.
- S. Dhakal and J. V. Selinger, "Statistical mechanics of splay flexoelectricity in nematic liquid crystals," *Phys. Rev. E* **81**, 031704 (2010).
- S. M. Shamid, S. Dhakal, and J. V. Selinger, "Statistical mechanics of bend flexoelectricity and the twist-bend phase in bent-core liquid crystals," *Phys. Rev. E* **87**, 052503 (2013).
- Z. Parsouzi, S. M. Shamid, V. Borshch, P. K. Challa, A. R. Baldwin, M. G. Tamba, C. Welch, G. H. Mehl, J. T. Gleeson, A. Jakli, O. D. Lavrentovich, D. W. Allender, J. V. Selinger, and S. Sprunt, "Fluctuation modes of a twist-bend nematic liquid crystal," *Phys. Rev. X* **6**, 021041 (2016).
- S. M. Shamid, D. W. Allender, and J. V. Selinger, "Predicting a polar analog of chiral blue phases in liquid crystals," *Phys. Rev. Lett.* **113**, 237801 (2014).
- L. Longa and G. Pająk, "Modulated nematic structures induced by chirality and steric polarization," *Phys. Rev. E* **93**, 040701 (2016).
- L. Longa and W. Tomczyk, "Twist-bend nematic phase in the presence of molecular chirality," *Liq. Cryst.* **45**, 2074–2085 (2018).
- G. Pająk, L. Longa, and A. Chrzanoska, "Nematic twist-bend phase in an external field," *Proc. Natl. Acad. Sci. U. S. A.* **115**, E10303–E10312 (2018).
- M. Čopič and A. Mertelj, "Q-tensor model of twist-bend and splay nematic phases," *Phys. Rev. E* **101**, 022704 (2020).
- E. G. Virga, "Double-well elastic theory for twist-bend nematic phases," *Phys. Rev. E* **89**, 052502 (2014).
- G. Barbero, L. R. Evangelista, M. P. Rosseto, R. S. Zola, and I. Lelidis, "Elastic continuum theory: Towards understanding of the twist-bend nematic phases," *Phys. Rev. E* **92**, 030501 (2015).
- R. S. Zola, G. Barbero, I. Lelidis, M. P. Rosseto, and L. R. Evangelista, "A continuum description for cholesteric and nematic twist-bend phases based on symmetry considerations," *Liq. Cryst.* **44**, 24–30 (2017).
- I. Lelidis and G. Barbero, "Nematic phases with spontaneous splay-bend deformation: Standard elastic description," *Liq. Cryst.* **43**, 208–215 (2016).
- E. I. Kats and V. V. Lebedev, "Landau theory for helical nematic phases," *JETP Lett.* **100**, 110–113 (2014).
- T. C. Lubensky and L. Radzihovsky, "Theory of bent-core liquid-crystal phases and phase transitions," *Phys. Rev. E* **66**, 031704 (2002).

- ¹⁹C. Greco and A. Ferrarini, "Entropy-driven chiral order in a system of achiral bent particles," *Phys. Rev. Lett.* **115**, 147801 (2015).
- ²⁰C. Greco, G. R. Luckhurst, and A. Ferrarini, "Molecular geometry, twist-bend nematic phase and unconventional elasticity: A generalised Maier-Saupe theory," *Soft Matter* **10**, 9318–9323 (2014).
- ²¹A. Ferrarini, "The twist-bend nematic phase: Molecular insights from a generalised Maier-Saupe theory," *Liq. Cryst.* **44**, 45–57 (2017).
- ²²W. Tomczyk, G. Pająk, and L. Longa, "Twist-bend nematic phases of bent-shaped biaxial molecules," *Soft Matter* **12**, 7445–7452 (2016).
- ²³A. Matsuyama, "Director-pitch coupling-induced twist-bend nematic phase," *J. Phys. Soc. Jpn.* **85**, 114606 (2016).
- ²⁴A. Matsuyama, "Twist-bend nematic phases in binary mixtures of banana-shaped liquid crystalline molecules," *Liq. Cryst.* **45**, 607–624 (2018).
- ²⁵A. Matsuyama, "Cholesteric-isotropic phase transitions of banana-shaped liquid crystalline molecules," *Mol. Cryst. Liq. Cryst.* **683**, 3–13 (2019).
- ²⁶M. A. Osipov and G. Pająk, "Polar interactions between bent-core molecules as a stabilising factor for inhomogeneous nematic phases with spontaneous bend deformations," *Liq. Cryst.* **44**, 58–67 (2017).
- ²⁷M. Cestari and A. Ferrarini, "Curvature elasticity of nematic liquid crystals: Simple matter of molecular shape? Insights from atomistic modeling," *Soft Matter* **5**, 3879–3887 (2009).
- ²⁸M. Cestari, E. Frezza, A. Ferrarini, and G. R. Luckhurst, "Crucial role of molecular curvature for the bend elastic and flexoelectric properties of liquid crystals: Mesogenic dimers as a case study," *J. Mater. Chem.* **21**, 12303–12308 (2011).
- ²⁹C. Greco, A. Marini, E. Frezza, and A. Ferrarini, "From the molecular structure to spectroscopic and material properties: Computational investigation of a bent-core nematic liquid crystal," *ChemPhysChem* **15**, 1336–1344 (2014).
- ³⁰P. De Gregorio, E. Frezza, C. Greco, and A. Ferrarini, "Density functional theory of nematic elasticity: Softening from the polar order," *Soft Matter* **12**, 5188–5198 (2016).
- ³¹Y. Yang, G. Chen, L. J. Martinez-Miranda, H. Yu, K. Liu, and Z. Nie, "Synthesis and liquid-crystal behavior of bent colloidal silica rods," *J. Am. Chem. Soc.* **138**, 68–71 (2016).
- ³²Y. Yang, H. Pei, G. Chen, K. T. Webb, L. J. Martinez-Miranda, I. K. Lloyd, Z. Lu, K. Liu, and Z. Nie, "Phase behaviors of colloidal analogs of bent-core liquid crystals," *Sci. Adv.* **4**, eaas8829 (2018).
- ³³F. Hagemans, R. K. Pujala, D. S. Hotie, D. M. E. Thies-Weesie, D. A. M. De Winter, J. D. Meeldijk, A. Van Blaaderen, and A. Imhof, "Shaping silica rods by tuning hydrolysis and condensation of silica precursors," *Chem. Mater.* **31**, 521–531 (2019).
- ³⁴C. Fernández-Rico *et al.*, "Shaping colloidal bananas to reveal biaxial, splay-bend nematic and smectic phases" (unpublished).
- ³⁵L. Onsager, "The effects of shape on the interaction of colloidal particles," *Ann. N. Y. Acad. Sci.* **51**, 627–659 (1949).
- ³⁶M. Chiappini, T. Drwenski, R. van Roij, and M. Dijkstra, "Biaxial, twist-bend, and splay-bend nematic phases of banana-shaped particles revealed by lifting the "smectic blanket", " *Phys. Rev. Lett.* **123**, 068001 (2019).
- ³⁷A. Mertelj, L. Cmok, N. Sebastián, R. J. Mandle, R. R. Parker, A. C. Whitwood, J. W. Goodby, and M. Čopič, "Splay nematic phase," *Phys. Rev. X* **8**, 041025 (2018).
- ³⁸N. Chaturvedi and R. D. Kamien, "Mechanisms to splay-bend nematic phases," *Phys. Rev. E* **100**, 022704 (2019).
- ³⁹P.-G. de Gennes and J. Prost, *The Physics of Liquid Crystals* (Oxford University Press, 1993).
- ⁴⁰P. G. D. Gennes, "Short range order effects in the isotropic phase of nematics and cholesterics," *Mol. Cryst. Liq. Cryst.* **12**, 193–214 (1971).
- ⁴¹E. F. Gramsbergen, L. Longa, and W. H. de Jeu, "Landau theory of the nematic-isotropic phase transition," *Phys. Rep.* **135**, 195–257 (1986).
- ⁴²L. Longa, D. Monselesan, and H.-R. Trebin, "An extension of the Landau-Ginzburg-de Gennes theory for liquid crystals," *Liq. Cryst.* **2**, 769–796 (1987).
- ⁴³G. J. Vroege and H. N. W. Lekkerkerker, "Phase transitions in lyotropic colloidal and polymer liquid crystals," *Rep. Prog. Phys.* **55**, 1241–1309 (1992).
- ⁴⁴J. C. Everts, M. T. J. M. Punter, S. Samin, P. van der Schoot, and R. van Roij, "A Landau-de Gennes theory for hard colloidal rods: Defects and tactoids," *J. Chem. Phys.* **144**, 194901 (2016).
- ⁴⁵R. Wittkowski, H. Löwen, and H. R. Brand, "Derivation of a three-dimensional phase-field-crystal model for liquid crystals from density functional theory," *Phys. Rev. E* **82**, 031708 (2010).
- ⁴⁶K. Schiele and S. Trimper, "On the elastic constants of a nematic liquid crystal," *Phys. Status Solidi B* **118**, 267–274 (1983).
- ⁴⁷C. W. Oseen, "The theory of liquid crystals," *Trans. Faraday Soc.* **29**, 883–899 (1933).
- ⁴⁸F. C. Frank, "I. Liquid crystals. On the theory of liquid crystals," *Discuss. Faraday Soc.* **25**, 19–28 (1958).
- ⁴⁹J. C. Tolédano and P. Tolédano, *The Landau Theory of Phase Transitions* (World Scientific, 1987).
- ⁵⁰R. van Roij, "The isotropic and nematic liquid crystal phase of colloidal rods," *Eur. J. Phys.* **26**, S57–S67 (2005).
- ⁵¹R. F. Kayser and H. J. Raveché, "Bifurcation in Onsager's model of the isotropic-nematic transition," *Phys. Rev. A* **17**, 2067–2072 (1978).
- ⁵²S. Kirkpatrick, C. D. Gelatt, and M. P. Vecchi, "Optimization by simulated annealing," *Science* **220**, 671–680 (1983).